International Journal of GEOMATE, March., 2023, Vol.24, Issue 103, pp.60-67
ISSN: 2186-2982 (P), 2186-2990 (O), Japan, DOI: https://doi.org/10.21660/2023.103.3699
Geotechnique, Construction Materials and Environment

VISUALIZATION OF HYDROPHOBIC COMPOUND DISTRIBUTION IN HARDENED CEMENT PASTE USING X-RAY CT

Yuto Fukdua[1], Feng Zhang[2], Nguyen Duc Van[3], and *Yukio Hama[4]

[1,2]Division of Sustainable and Environmental Engineering, Muroran Institute of Technology, Japan; [3]College of Environmental Technology, Graduate School of Engineering, Muroran Institute of Technology, Japan; [4] College of Design and Manufacturing Technology, Muroran Institute of Technology, Japan

*Corresponding Author, Received: 15 Nov. 2022, Revised: 17 Jan. 2023, Accepted: 10 Feb. 2023

ABSTRACT: Although hydrophobic compounds have been reported as an effective method for improving frost resistance of concrete, little research has been undertaken to investigate the behavior of hydrophobic compounds in hardened cement paste (HCP). Moreover, by using the existing cross-sectional observation approach to investigate the air void system in HCP, it is unclear how oil droplets exist in the HCP, and distinguishing between air bubbles and droplets becomes difficult. In this study, silicone oil and paraffin were used as the hydrophobic compounds. The behavior of silicone oil and paraffin in the HCP was investigated using X-ray computer tomography (CT) as a non-destructive method to elucidate the mechanism of suppressing frost damage. The findings demonstrated that it is clearly possible to distinguish between oil droplets and air bubbles in the HCP containing silicone oil. Furthermore, we could also observe how oil droplets disappeared and changed into voids during the hardening process. In contrast, the HCP containing a paraffin admixture was unable to distinguish between air bubbles and paraffin.

Keywords: Frost resistance, Hydrophobic compounds, X-ray CT, Setting and Hardening

1. INTRODUCTION

Frost damage to concrete is a serious deterioration phenomenon that occurs in cold regions and causes a loss of strength and aesthetic appeal. Research is being conducted daily on how to improve the frost resistance of concrete. It is known that sufficient entrained air is important to improve frost resistance, and efforts are being made to ensure a relatively large amount of entrained air during mixing in anticipation of a decrease in air volume due to vibratory compaction [1,2]. Therefore, not only the Japanese standards [3,4] but also the standards of other countries such as South Korea [5], China [6,7], the United States [8,9], and Europe [10] prescribe that more air must be introduced if there is a risk of frost damage than when there is no risk of frost damage. However, there is a problem that it is difficult to control a large amount of air content during mixing concrete, and an excessive amount of air content leads to a decrease in compressive strength [3].

On the other hand, the frost resistance of concrete may be significantly reduced due to drying and other factors [11]. This can be improved with entrained air. However, considering the aforementioned disadvantage of a reduction in compressive strength due to entrained air, an alternative method for improving frost resistance without the contribution of entrained air is essential. The addition of a hydrophobic compound has been reported as an effective method for improving the frost resistance of concrete. Honda et al. [12] reported that the addition of paraffin as a hydrophobic compound to mortar would improve its resistance to frost damage. Kishimoto et al. [13,14] suggested that the addition of an appropriate amount of silicone oil also improved frost resistance. The results showed that the amount of air bubbles increased with the addition of the hydrophobic compound (see Fig.1). The results also indicated that the addition of the hydrophobic compound did not make a significant difference in the air content of fresh mortar. Meanwhile, an increase in the air content of hardened mortar was obtained compared to that of fresh mortar. As shown in Fig.1, the air bubbles were considered to be oil droplets created by the hydrophobic compounds finely dispersed in the hardened cement paste (HCP) [15]. It is explained that the inter-bubble spacing coefficient (including oil droplets) became smaller as the oil droplets behaved as air bubbles in the HCP. However, the current cross-section observation method includes a step of cutting the sample, which discharges oil droplets. It is difficult to distinguish between air bubbles and oil droplets. Furthermore, this method cannot clearly explain the existence of the oil droplets in the hardened cement.

In recent years, a non-destructive X-ray computer tomography (CT) method has been attracting great attention in cement-based materials, including internal pore structure analysis with a three-dimensional characterization of materials. X-ray CT is an observation method that irradiates an

object with X-rays, captures multiple 2-dimensional images generated by the transmitted X-rays while rotating the object, and reconstructs them into three-dimensional data through numerical processing. Temmyo et al. [16] proposed a method for quantifying the material composition of concrete using X-ray CT. Jiande et al. [17] simulated the carbonation process of concrete based on the in-situ microstructure evolution of X-ray CT. In addition, Cnudde et al. [18] compared and discussed the advantages and disadvantages of porosity data obtained from three techniques, including MIP, X-ray CT, and water absorption under vacuum. The microstructure of mortar was investigated using X-ray CT [19, 20]. These studies demonstrate that the observation using the X-ray CT method can allow the cross-sectional observation of oil droplets trapped in the HCP.

Therefore, the main objective of this research is to three-dimensionally visualize the distribution of oil droplets in the HCP containing paraffin (P) and silicone oil (SO) as the hydrophobic compounds using the X-ray CT method. There are also some research questions that will be addressed in this study, namely: How do the hydrophobic compounds exist in the HCP as oil droplets? How do these oil droplets change during the hardening process of the cement paste?

To address the questions raised above, we visualize the HCP without admixtures, air, and hydrophobic compounds as a single phase to distinguish them based on the color results of materials after scanning. Then the HCP containing the hydrophobic compounds was scanned to observe the existence of the hydrophobic compounds. Finally, the change in hydrophobic compound in the HCP was observed during the hardening process of cement paste.

2. MECHANISM OF INHIBITION OF FROST RESISTANCE OF HYDROPHOBIC COMPOUNDS

Powers [21] reported that interior structures are destroyed by the pressure of the antifreeze agent generated during the freezing process, despite the fact that the antifreeze agent has been widely utilized to suppress freezing deterioration. It is common knowledge that water expands by around 9% in volume when it freezes. The unfrozen water will therefore pass through the pore structure of the hardened cement paste as a result of its volume expansion when the water in the concrete freezes. Because the dense pore structure in the hardened cement paste creates viscous resistance when water moves through it, a gradient of hydraulic pressure is created. Concrete begins to crack and deteriorate when the hydraulic pressure created exceeds the concrete's tensile strength. A conceptual diagram and theoretical formula for the production of hydraulic pressure are shown in Fig.2. Based on this, Katsura et al. proposed a model for the frost damage mechanism of HCP [22], which is shown in Eq (1).

$$P = \frac{8\eta G l}{n\pi r^4} \qquad (1)$$

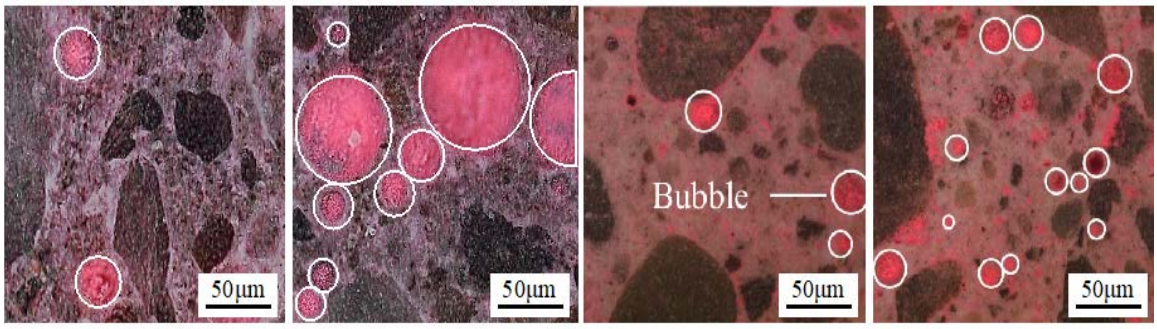

Paraffin 0% Paraffin 2.7% Silicone Oil 0% Silicone Oil 5%

Fig.1 Cross-sectional photographs of concrete containing the hydrophobic compounds [12,14]

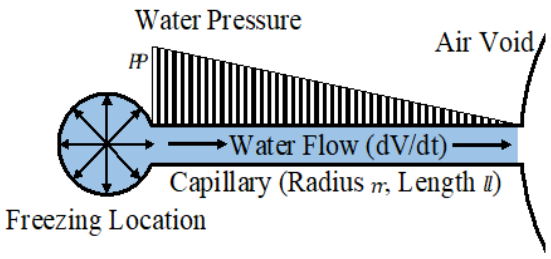

Fig.2 Conceptual diagram and theoretical formula for generation of water pressure [12]

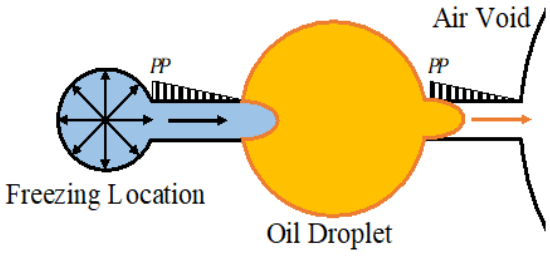

Fig.3 Diagram of mechanism of suppression of frost damage by a hydrophobic compound [12]

Table 1 Physical properties of materials

Classification	Physical properties
Cement	Ordinary Portland cement, Density: 3.16g/m^3, Specific surface area: 3500cm^2/g
Water	Tap water in Muroran Institute of Technology
AE Admixture	Alkyl ether system, Anion
Paraffin	Paraffin emulsion, Density: 0.98g/cm^3
Silicone Oil	Density: 0.96g/cm^3

Table 2 Experimental plan

Sample	Cement	w/c (%)	Admixture (C×wt.%)			Measuring conditions for X-Ray CT		
			AE	Paraffin	Silicone Oil	Resolution (μm)	Suga voltage (kV)	Frame averaging
N	OPC	50	-	-	-	8.2	100	3
AE			0.004	-	-			
P			-	2.7	-			
SO			-	-	2.7			

where,
$\boldsymbol{P}$ is water pressure (N/m^2);
$\boldsymbol{\eta}$ is viscosity coefficient of liquid (N/m^2);
G is flow velocity (m^3/s);
L is distance between freezing location and air void (m);
N is number of capillaries connecting to air void;
r is radius of capillary (m).

The damage occurs when the water pressure P exceeds the tensile strength of the HCP, and this equation also indicates that P is affected by the distance between the freezing location and the air void. Based on this model, Nishi et al. [15] reported that hydrophobic compounds are finely dispersed as oil droplets in the HCP and decrease the water pressure by shortening the distance between the freezing location and the air void, thereby suppressing the frost damage. However, they also reported that the penetration space of water reaching the oil droplets is only the volume change with the decreasing temperature, and that alone cannot relieve pressure via the 9% volume expansion due to the water freezing. By considering that the oil droplets have the same viscosity as water and are movable, Honda et al. [12] proposed a hypothesis that the hydrophobic compound existing as oil droplets in the HCP will be pushed out of space by the water pressure, as shown in Fig.3. This could be accomplished by decreasing the flow distance of water and providing a space for water to freeze, which would reduce the water pressure, thereby suppressing the frost damage.

3. EXPERIMENTAL PROGRAM

3.1 Materials and Specimen Preparation

Table 1 shows the properties of the material used in this study. Ordinary Portland cement and tap water were used to prepare the hardened cement paste. The paraffin waterproofing agent and silicone oil were used as the hydrophobic compounds. The air-entraining (AE) agent was added to the cement paste to evaluate the difference between air voids and oil droplets.

In order to take images with the highest possible resolution, the cement paste was cast into the thin plastic straws with an inner diameter of 8 mm. The X-ray CT test was performed without demolding because the thin plastic straw was considered to have little effect on the results during measurements.

3.2 Experimental design

In this study, three parts of experiments were performed.

In Part 1, the phases in the HCP were identified based on the different gray levels of materials. In the CT images, the materials with a high density and atomic number that are difficult for X-rays to penetrate are displayed in white, while materials with a low density and atomic number that are easily penetrated are displayed in black. In this part, an experiment was performed to identify the HCP, pores, and hydrophobic compounds (paraffin, silicone oil). The single object was cast in the plastic tube with three levels before the X-ray CT test, as shown in Fig.4.

Based on the experimental results of Part 1, Part 2 is aimed at observing the existence of paraffin and silicone oil in the HPC. In this study, four specimens of cement paste were made with and without admixtures such as AE agent, P, and SO. Table 2 presents the experimental design. The HCP specimens were scanned at the age of 2 days.

In Part 3, the HCP specimens were scanned at different ages (0.5, 1, 2, 4, 6, 8, 10, and 35 hours) to observe the change of P and SO in the HCP during

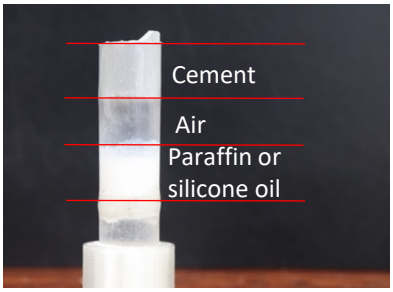

Fig.4 Experiment for identifying the phases

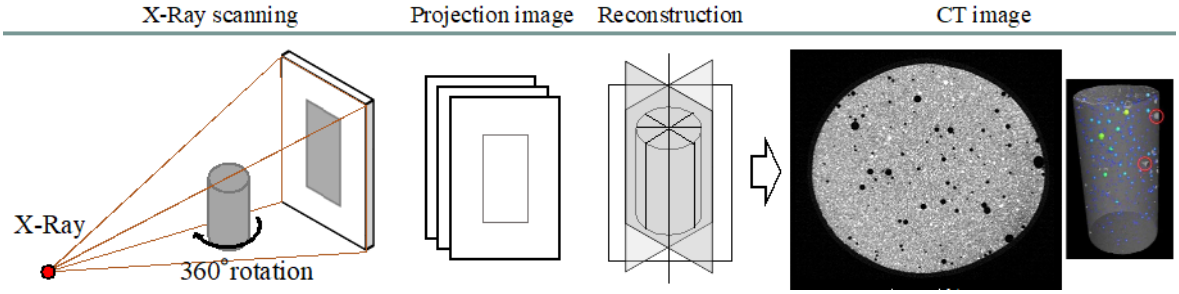

Fig.5 X-ray CT scanning and imaging process

the hardening process. Additionally, the volume of oil droplets and air voids were also calculated using the VGSTUDIO MAX software.

3.3 X-ray CT test

An industry device of X TH 225 and X TH 320 with an X-ray source of 225 kV was used in this word. This technique uses the fundamental principle of the interactions between X-rays and materials when the specimen is bombarded by an X-ray beam and the transmitted beam is recorded on the detector. Based on Beer-Lambert's law, the attenuation of X-rays can be calculated using the following equation:

$$I = I_o e^{-\mu x} \quad (2)$$

where,
I is the intensity of the reflected X-rays (Wm^{-2});
I_o is the intensity of the incident X-ray (Wm^{-2});
x is the material thickness in the direction of X-ray transmission (m);
μ is the linear attenuation coefficient, which is dependent on the density, X-ray energy, and atomic number of the material (m^{-1}).

In this way, the CT makes it possible to volumetrically measure the attenuation and absorption of X-rays through the materials and create an image that maps changes in the attenuation coefficient within the volume.

In this study, the specimen of HCP is rotated 360 degrees in the horizontal direction, and a series of X-ray transmission images are recorded, as shown in Fig.5. For this test, the resolution, voltage of the X-ray tube, and frame averaging were 8.2 μm, 100 kV, and 3, respectively.

4. RESULTS AND DISCUSSION

4.1 Identifying specimen phases

Fig.6 shows the representative X-ray projections of the HCP (without admixtures), air, and only paraffin or silicone oil. As can be seen in Fig., the white and dark colors represent the phases of cement matrix and air, respectively. Meanwhile, the gray and bright gray show the phases of paraffin and silicone oil. This may be due to the fact that P and SO have the same density, but the number of atoms constituting SO is larger than that of P.

4.2 Visualization of hydrophobic compounds in hardened cement

Fig.7 shows the horizontal images of the HCP specimens with and without admixture such as AE agent, paraffin and silicone oil and the 3D structure of air void at the age of 2 days. According to the results of identifying the phases above, it is clear that the black areas present the air void in the HCP. As shown in Fig.7, compared with specimen N, the content of air void in the HCP specimen mixed with AE, P, SO was larger. This tendency is easer However, the air void size in the HCP specimen containing AE was smaller than that of specimen containing P and SO. Nishi et al. [15] assumed that the hydrophobic compounds existed saturated in the pore as oil droplets. However, from the sectional X-

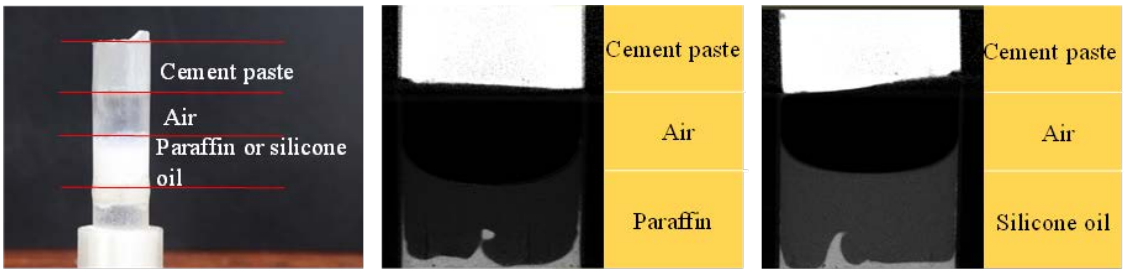

Fig.6 2D slices from X-ray CT identifying specimen phases in a vertical

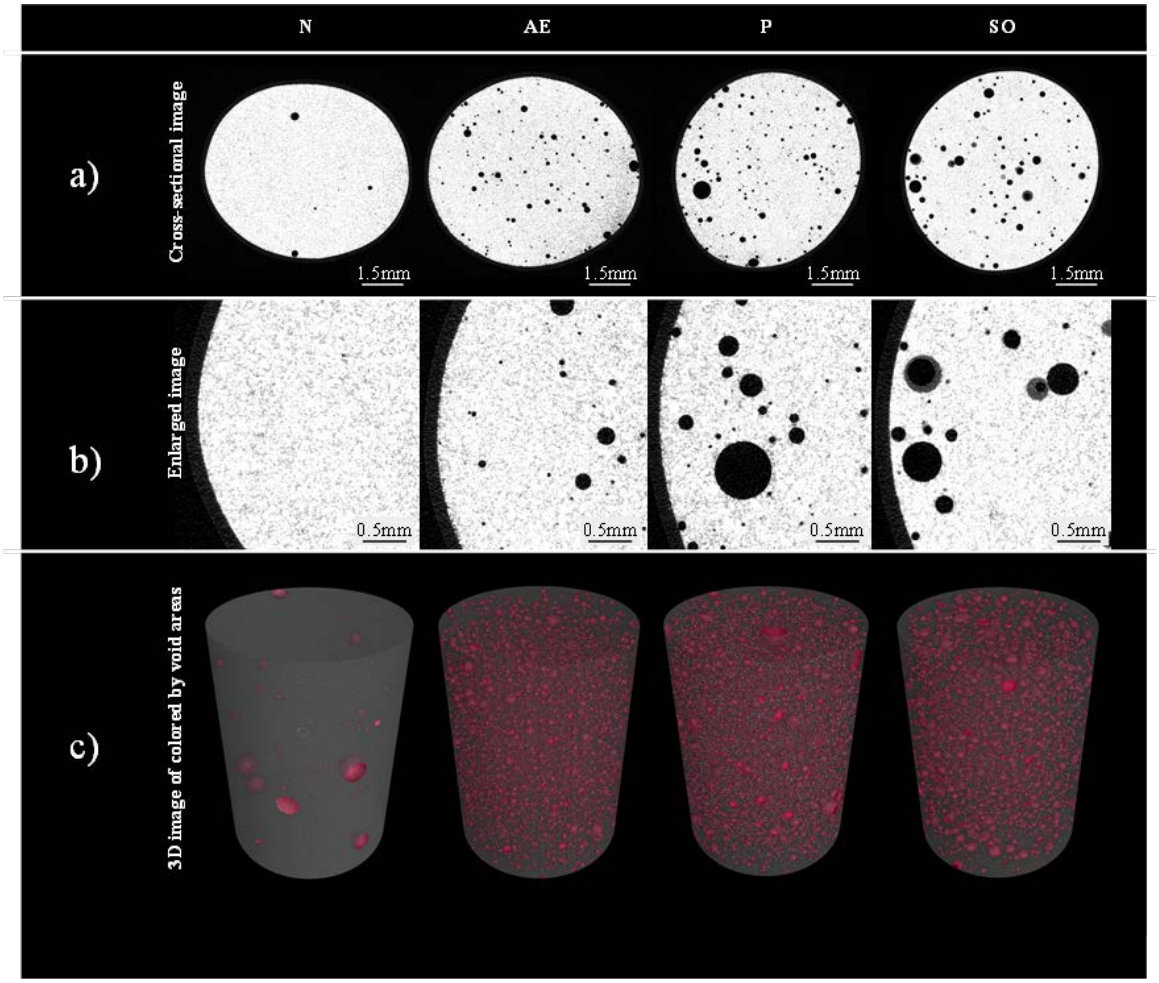

Fig.7 Selected horizontal sectional X-ray CT images (a, b) and 3D structure of air void in HCP (c).

ray CT images of the P and SO specimen, the black area was considered to be air bubbles rather than oil droplets. In the case of the HCP containing SO, the light gray areas were observed on the pore wall (see Fig.7b). This indicated that the SO existed in the pore and adhered on the surface of pore wall as an oil film. Meanwhile, in the case of the HCP containing P, the gray areas were not observed in the cross-sectional X-ray CT image (see Fig.7b) and all the black areas were considered to be pores. This may be explained by two reasons. First, Paraffin is weakly sensitive in identifying by X-ray, therefore, it could be identified when the scan was performed on P as a single phase (see Fig.6). However, it is difficult to identify P that exists in the other phases (such as cement matrix). Second, unlike in the case of SO, the paraffin may exist in the cement matrix instead of in the pores. However, it should be reflected as air content in the air content test of the fresh mortar or concrete. Therefore, more verifications of paraffin admixtures are necessary for the future.

4.3 Observation of change of hydrophobic compounds in early age hardening process

Because no oil droplets were seen for the specimens containing the hydrophobic compounds, it is expected that the air content of the specimens will increase by the same amount as that of the

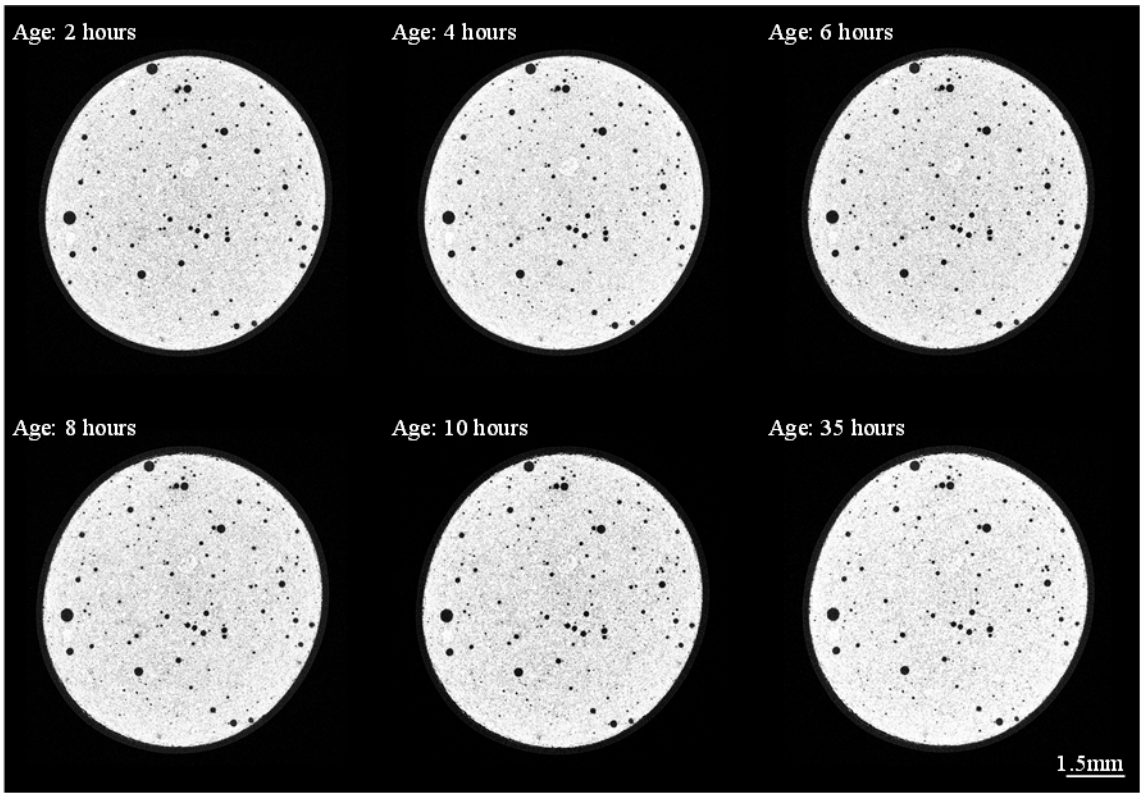

Fig.8 The early age hardening process for P

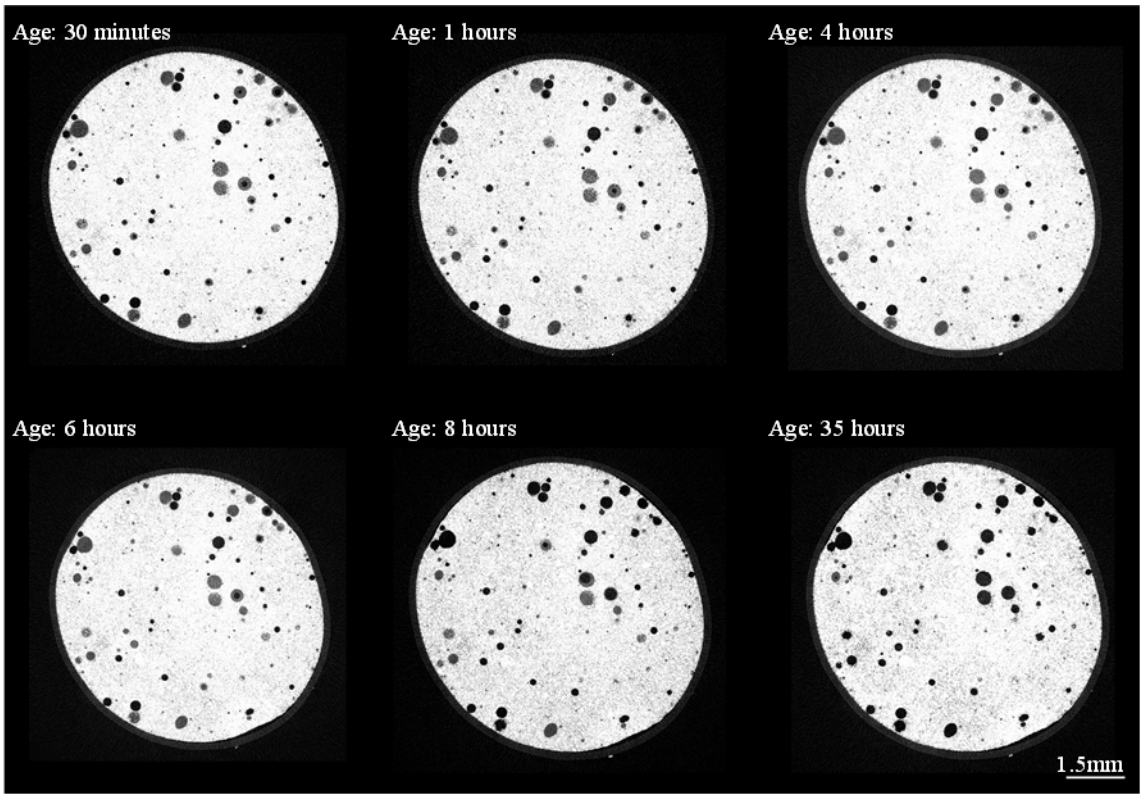

Fig.9 The early age hardening process for SO

specimens added with the AE agent (see Fig.1). However, this statement is not in line with the findings of Honda et al., who showed the relationship between the air content of fresh and hardened concrete. The result showed the air content of hardened concrete is higher than that of

fresh concrete. Therefore, we presumed that the behavior of the hydrophobic compounds may be changed immediately after the casting and hardening processes. In this section, to observe the change of the hydrophobic compounds in the hardening process of cement paste, the specimens will be scanned at an early age. Figs.8 and 9 comparatively display the sectional X-ray CT images of the specimens containing P and SO at the early and late stages of the hardening process, respectively. As shown in Fig.8, the black areas were considered as the pores, which were observed immediately after casting cement paste on the plastic straw. Furthermore, these black areas almost did not change with time. Especially, no paraffin-like substance was observed. This observation is consistent with the above result (see Fig.7). Meanwhile, in the case of SO, the gray areas were observed immediately after pouring cement paste into the plastic straw. It is clear that the gray areas inversely changed to the black ones with the hardening process of the cement paste. This indicated that the pores were saturated by SO as the oil droplets formed in the initial time of casting, then with the passage of time, oil droplets became the pores.

Additionally, the difference in the air content of fresh and hardened cement paste was calculated, as shown in Fig.10. The results showed that the volume of the oil droplet gradually decreased, while that of the air bubble increased with time. It can also be seen that the volume of the oil droplets plus air bubbles is almost constant from the beginning. Here, the amount of silicone oil added was 2.7% relative to the mass of cement, which was 3.4% when converted to unit volume. This was almost the same as the number of oil droplets (approximately 3.6%) calculated by X-ray CT after casting the cement paste. The results also indicated that the volume of oil droplets decreased from 6 to 8 hours. Furudate et al. [23] reported that the hardening of cement started at 7.5 h with a w/b of 0.5, leading to the formation of capillary pores. This caused the movement of silicone oil from air bubbles into the capillary pores. This also explains why the gray areas become the black areas (see Fig.9). Therefore, it can be concluded that the places of oil droplets

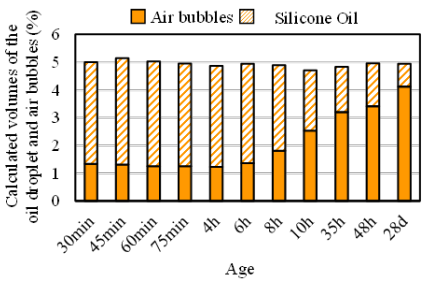

Fig.10 Calculated volume of the oil droplet and air bubble in the HCP containing SO

will become empty pores and behave as air bubbles.

It is also conceivable that the migration behavior of water in the capillary pores during freezing may be changed due to the migration of the silicone oil into the capillary pores.

5. CONCLUSION

In this study, in order to elucidate the mechanism by which hydrophobic compoundsimprove frost damage resistance, experiments were conducted to visualize the distribution of hydrophobic compounds in hardened cement paste using X-ray CT. The following major conclusions are drawn based on the X-ray CT test results and discussion:

(1) The X-ray CT images directly and visually observe the increase in the porosity of the HCP due to the addition of hydrophobic compounds in three dimensions.

(2) Silicone oil exists in the cement paste as oil droplets immediately after casting and moves into the capillary pores that will form when the hardening process begins. After moving, the places where oil droplets once were will become air bubbles, which contributes to the improvement of frost resistance.

(3) It is difficult to observe paraffin in the cement paste during the hardening process. This can be explained by two possible reasons. First, paraffin reacts weakly to X-rays and is difficult to find in complex phases like the HCP. Second, paraffin may exist in the cement matrix instead of air bubbles as in the case of silicone oil. For the second reason, the air content in fresh conditions must be consistent with that in hardened conditions. However, this hypothesis is not consistent with the findings of Honda et al. Therefore, in the future, more investigations will be necessary for the verification of paraffin admixtures.

6. REFERENCES

[1] Wong H.S., Pappas A.M., Zimmerman R.W., Buenfeld N.R., Effect of entrained air voids on the microstructure and mass transport properties of concrete, Cement Concrete Research, 41, 2011, pp. 1067-1077.

[2] Yuan J., Wu Y., Zhang J., Characterization of air voids and frost resistance of concrete based on industrial computerized tomographical technology, Const. Build. Mat., 168, 2018, pp. 975-983.

[3] Japanese Architectural Standard Specification JASS 5 Reinforced Concrete Work, 2018.

[4] Japanese Industrial Standards, Ready-mixed concrete, JIS A 5308, Japanese Standards Association, Tokyo, Japan, 2019.

[5] Korean Industrial Standards, Ready-mixed concrete, KS F 4009, Korean Standards Association, Seoul, Korea, 2016.
[6] Chinese National Standard, Specification for mix proportion design of ordinary concrete, JGJ 55, China, 2011.
[7] Chinese National Standard, Ready-mixed concrete, GB/T 14902, China State Bureau of Quality and Technical Supervision, China, 2012.
[8] American Concrete Institute, Standard practice for selecting proportions for normal, heavyweight, and mass concrete, ACI 211, State of Michigan, America, 2009.
[9] ASTM International, Standard specification for ready-mixed concrete, ASTM C 94, American National Standards Institute, Commonwealth of Pennsylvania, America, 2020.
[10] European Standard, Concrete - Specification, performance, production and conformity, EN 206, European Committee for Standardization, European Union, 2013.
[11] Mitaka S., Hirano A., Ota K., Hama Y., Tabata M., Influence of spacing factor and distribution of air void diameter on frost resistance of high strength concrete, AIJ., 2005, pp. 1141-1142.
[12] Honda D., Quy N.X., Kim J., Hama Y., Influence of drying on frost resistance of mortar using a nitrite corrosion inhibitor and paraffin waterproofing agent, Const. Build. Mat., Vol. 283, 2021, 122581.
[13] Kishimoto G., Kim J., Choi H., Hama Y., Influence of Silicone Oil on Durability of Portland Blast Furnace Slag Cement Mortar, Advanced Concrete Technology Vol.16, 2018, pp.110-123.
[14] Kishimoto G., Yasuda R., Choi H., Hama Y., Study on the Mechanism of reduction of Frost Resistance of Mortar containing Silicone oil, Japan Concrete Institute, 40, 2018, pp.825‑830.
[15] Nishi H., Nawa T., Study on frost damage degradation in hydrated cement using hydrophobic compound, J. Struct. Constr. Eng. AIJ., Vol.79, 2014, pp. 1415- 1424.
[16] Temmyo T., Ito G., Hamazaki T., Proposal of quantitative method for material composition of concrete by x-ray CT method Japan Concrete Institute, Vol.30, No.2, 2008.
[17] Jiande H., Weiqing L., Shuguang W., Dongsheng D., Feng X., Weiwei L., Schutter G.D., Effects of crack and ITZ and aggregate on carbonation penetration based on 3D micro-X-ray CT microstructure evolution, Const. Build. Mat., Vol.128, 2016, pp. 256-271.
[18] Cnudde V., Cwirzen A., Masschaele B., Jacobs P.J.S., Porosity and microstructure characterization of building stones and concretes, Engineering Geology, Vol.103, 2009 pp. 76-83.
[19] Hitomi T., Mita Y., Saito Y., Takeda N., Observation of the microstructure of mortar using X-ray CT images at SPring-8 (in Japanese) Japan Concrete Institute, Vol.26, No.1, 2004.
[20] Sugiyama T., Shimura K., Hatakeda D., Investigation of Pore Structures in AE Mortar Using High-Resolution-Type X-ray CT, Journal of JSCE E2, Vol.67, No.3, 2011, pp. 351-360.
[21] Powers T.C., A working hypothesis for further studies of frost resistance of concrete, J. Proc. ACI., Vol.41, 1945, pp. 245–272.
[22] Katsura O., Yoshino T., Kamata E., A model for mechanism of frost damage of cementitious material, Concr. Res. Technol. 11 (2), 2000, pp. 49–62.
[23] Furudate M., Yamashita K., Kim J., Hama Y., Slowdown of strength development of cement paste by freezing before and after the start of setting time, Japan Concrete Institute, Vol.41, No.1, 2019.